Simulation design and analysis of angle between outer and inner wings of flapping wing robot

Tong Wu[a], Bosong Duan[*b], Anyu Sun[b]
[a]Computer Application Institute of Nuclear Industry, China National Nuclear Corporation, Beijing 100822, China; [b]School of Mechanical Engineering, Zhejiang University, Hangzhou 310027, Zhejiang, China

ABSTRACT

There is an obvious angle between the outer and inner wings of large birds during flight, gliding and landing, and the corresponding angle is different under different flight conditions. In this paper, the influence of different outer and inner wing angles on aerodynamic characteristics is studied. Based on the existing bat-like flapping-wing aerial vehicle (FAV), a series of wing models with different outer and inner wing angles are established, then the aerodynamic characteristics are analyzed by XFlow-Abaqus co-simulation, and the simulation results are verified by wind tunnel experiment. The results show that lift increases first and then decreases with the increase of the angle between the outer and inner wing, and the maximum lift can be obtained when the angle is 15°, compared with the angle of 0°, the lift increase is about 10%, the thrust and the pitch moment decrease with the increase of the angle. The research in this paper provides theoretical guidance for the wing structure optimization of flapping wing robots, and is helpful to the wing structure design and optimization of flapping wing robots.

Keywords: Flapping-wing aerial vehicle, outer and inner wing, flexible wing, fluid-structure interaction, wind tunnel experiment

1. INTRODUCTION

Over the past few decades, the development of new materials and micro-electromechanical technologies has driven the rapid advancement of aerial vehicles[1]. These vehicles now come in a variety of flight modes, including fixed-wing, rotary-wing, and flapping-wing designs[2]. Owing to their bionic shapes, many aerial vehicles possess good stealth, low noise, and high maneuverability[3], making them promising for both military reconnaissance and civilian applications[4].

Different from some insects[5,6] and small birds[7] whose wings are mostly fixed in shape, the wings of large birds such as bats[8], seagulls[9] and eagles[10] are divided into outer and inner wings, and the relationship between the two wings is similar to human arms and hands. The inner wing is connected with the body and is controlled by the body to flap, the outer wing is driven by the inner wing. The special structure of the outer and inner wings has attracted the research interest of many scholars, such as: Ang[11] analyzed the seagull wings flutter characteristics and constructed a new flexible wing model, enabling the outer wings to have a wider range of rotation angles. This structure can more truly simulate the flight attitude of seagulls and obtain higher lift under low frequency flapping. Huang[12] took a double-crank-rocker flapping wing mechanism as the research object to simulate the movement of the eagle's inner wing and outer wing. Through experiments, the inner wing is the key to generate lift while the outer wing is the key to generate thrust. Mahardika[13] designed a FAV with a separable outer wing to explore the application of wing feather separation in FAV. The experimental results show that the lateral deformation of the separated wing is large, the drag generated by the upper stroke is small, and the lift and thrust generated by the lower stroke are relatively large.

To sum up, relevant researches on FAV are carried out from the perspectives of structural characteristics of outer and inner wings, aerodynamic characteristics and advantages over single-wing structures. However, in practice, there is a certain angle between the outer and inner wing of large birds, and the angle between the outer and inner wing is different for different birds in different flight processes, as shown in Figure 1. What's more, the angle between the outer and inner

*bosongduan@zju.edu.cn

International Conference on Optics, Electronics, and Communication Engineering (OECE 2024), edited by Yang Yue, Proc. of SPIE Vol. 13395, 133950F · © 2024 SPIE · 0277-786X · Published under a Creative Commons Attribution CC-BY 3.0 License · doi: 10.1117/12.3049183

wings varies between different organisms and different flight processes. This biological phenomenon can still be preserved in thousands of years of biological evolution, indicating that it must be beneficial to flight.

Figure 1. Angle between the outer and inner wing of large birds.

In this paper, the influence of the angle between the outer and inner wings on the aerodynamic characteristics of flapping wing robots is studied. Firstly, the wing structure was analyzed, and several different wing models were constructed by changing the angle between the outer and inner wing. Then, XFlow-Abaqus were used for fluid-structure interaction (FSI), the simulation results of lift, thrust and pitch moment under the included angle of each wing were obtained. After that, the accuracy of simulation was verified by wind tunnel experiments. Finally, the results were compared and analyzed, and relevant conclusions were drawn about the effect of outer and inner wing angle on aerodynamic characteristics, and the application rules of outer and inner wing angle in FAV were summarized.

2. STRUCTURAL ANALYSIS OF OUTER AND INNER WING

Figure 2 shows the shape of bat wing in the actual movement process. It can be seen from the figure that the bat membrane is completely attached to the skeleton and is driven by the skeleton joint to produce movement deformation. The inner wing structure (the area composed of B1B4B9B10) of the wing, just like the human arm, contains the arm, elbow, forearm and other joints. The outer wing structure (the area of B4B7B8B9) is similar to the part of the human wrist and hand. The movement of the inner wing joint is driven by the shoulder to adjust the amplitude and frequency of the wing flapping, and then the outer wing is driven by the inner wing to realize the flight of the bat.

Figure 2. The structure of bat wing.

In addition to the flexible deformation of wing in Figure 2, it is obvious that there is an angle between the inner wing and the outer wing, and the influence of this angle on the aerodynamic characteristics of bat flight is the focus of this paper. First of all, the wing needs to be modeled according to the principle of bionics. The shape design of wings adopts bat bionics equations in Norberg's paper[14], as shown in equations (1) and (2):

$$B = 1.200m^{0.322} \tag{1}$$

$$S = 0.203m^{0.639} \tag{2}$$

where B is wingspan, S is the area of wing, m is mass of bat.

The definition of wing morphological parameters is shown in Figure 3. S_{hw} is the area of outer wing, S_{aw} is the area of inner wing. l_{hw} is the span length outer wing and l_{aw} is the span length of inner wing.

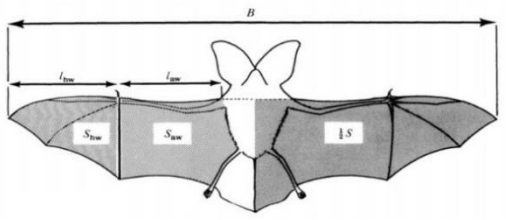

Figure 3. The definition of wing morphological parameters[14].

The aspect ratio λ of wings is:

$$\lambda = \frac{B^2}{S} \tag{3}$$

Aspect ratio is not enough to describe wing shape. S_{hw}, S_{aw}, l_{hw}, l_{aw} are used to describe wing shape.

Length ratio of outer wing to inner wing T_l and T_s is:

$$T_l = \frac{l_{hw}}{l_{aw}} \tag{4}$$

$$T_S = \frac{S_{hw}}{S_{aw}} \tag{5}$$

Wing shape index I does not depend on aspect ratio, but only depends on the relative size of outer wing and inner wing. A large value of I indicates that the wing is close to round or square. Assuming that the value of I is infinite, it corresponds to the rectangular wing. I=1 corresponds to the triangular wing; The smaller the I value, the sharper the wing becomes, and the chord becomes significantly smaller as it approaches the tip. Wing shape index I is:

$$I = \frac{T_S}{T_l - T_S} = \frac{1}{T_l/T_S - 1} \tag{6}$$

In this paper, through the data fitting of 88 groups of actual bats, the fitting results of T_l and I are shown in Figure 4.

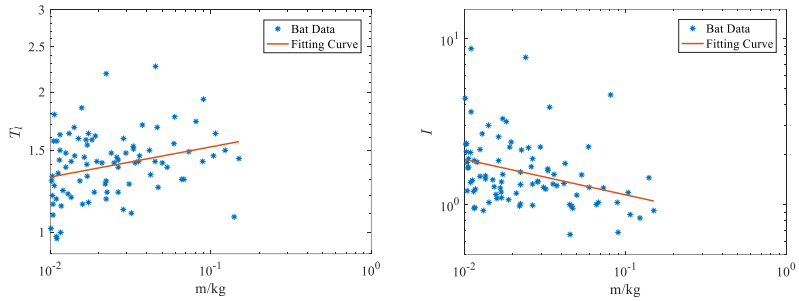

Figure 4. Fitting results of T_l and I.

The fitting results are shown in equations (7)-(10):

$$lgT_l = 0.0646lgm + 0.2480 \tag{7}$$

$$T_l = 1.77m^{0.0646} \tag{8}$$

$$lgI = -0.2132lgm - 0.1543 \tag{9}$$

$$I = 0.7001m^{-0.2132} \tag{10}$$

Finally, the chord length $c(r)$ of wings along the spanwise distribution is:

$$c(r) = \frac{S_{aw}}{l_{aw}}\left[1 - \left(\frac{r - l_{aw}}{l_{hw}}\right)^I\right] \tag{11}$$

Under the condition that the wing area remains unchanged, the included angle between the inner wing and the outer wing is changed to construct a set of wing models, as shown in Figure 5. The specified angle is positive clockwise and negative counterclockwise. The range of included angle is [-30°, 45°]. Through simulation analysis, it is found that the included

angle is within [0°, 20°], which will obtain better aerodynamic characteristics. Therefore, in order to ensure the accuracy of the results and save time, the value is density normal distribution. The specific angle values are [-30°, -25°, -20°, -15°, -10°, -5°, 0°, -2°, 3°, 4°, 5°, 8°, 10°, 13°, 14°, 15°, 16°, 18°, 20°, 25°, 30°, 45°].

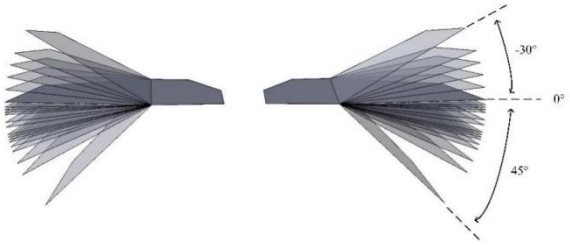

Figure 5. Models of different angle between outer and inner wings.

3. SIMULATION RESULTS AND ANALYSIS

In this paper, Abaqus-XFlow co-simulation is leveraged to calculate the aerodynamic forces acting on the wing. The XFlow software is responsible for observing the changes in the flow field and the aerodynamic forces experienced by the wing, and it then transmits the wing forces to the Abaqus software. Abaqus, in turn, monitors the deformation of the wing and feeds the deformation and movement data back to XFlow. This coupled simulation approach enables better replication of the real-world behavior of the wing. The wing material used is PDMS, which has a density of 1000 kg/m3, an elastic modulus of 2.3 MPa, and a Poisson's ratio of 0.4. Figure 6 illustrates the simulated wind tunnel setup for the calculations. Within the flow field area, the Z-axis is set as the direction of the freestream flow velocity, while the X-axis and Y-axis have no flow velocity. Additionally, the outlet boundary is defined as the freestream outflow with a velocity gradient of 0. To ensure the convergence of the results, the Courant number is set to 0.01. The particle size within the wind tunnel is set to 0.011, which is deemed sufficient to maintain the accuracy of the calculations. The flow field medium is chosen to be air at normal temperature, and the other simulation conditions include the maximum wing flapping angle of 30°, the flapping frequency of 3 Hz, the wing angle of attack of 15°, and the freestream flow velocity of 5 m/s.

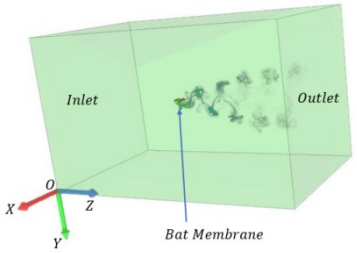

Figure 6. Simulated wind tunnel.

Figure 7 presents the curves of lift, thrust, and pitch moment obtained through flow field simulations under different angles between the outer and inner wings.

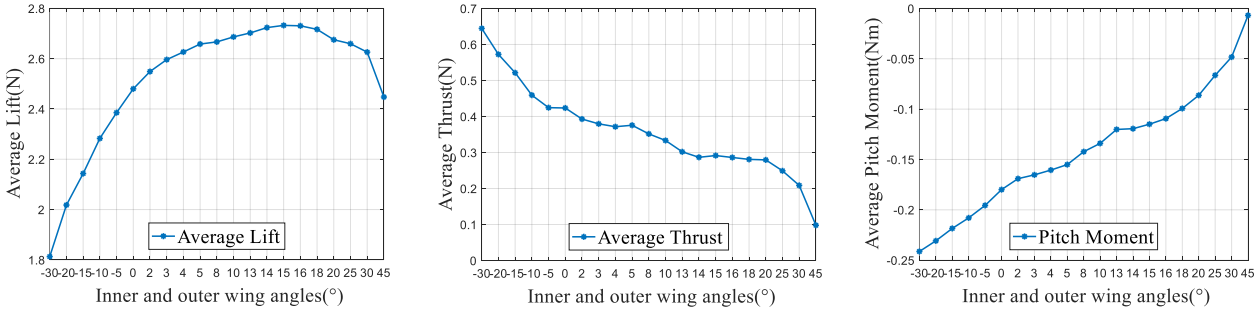

(a) Lift (b) Thrust (c) Pitch moment

Figure 7. Average lift, thrust and pitch moment corresponding to different outer and inner wing angles.

Figure 7 shows the Average lift, thrust and pitch moment corresponding to different outer and inner wing angles. It can be seen from Figure 7a that the average lift when the angle between outer and inner wings is positive is greater than that when the angle between outer and inner wings is negative. This is because although the area of each wing is the same, when the angle between outer and inner wings is positive, the effective area of interaction with air in the downward process is larger, so that more lift can be obtained. Through the curve, it is found that when the angle range is between [0°, 20°], the lift changes slowly, and when the angle between the outer and inner wings is 15°, the maximum lift is 2.732 N, which is 10.16% higher than the lift of the outer and inner wing angle is 0°. when the angle exceeds 20°, the lift shows a significant downward trend, because the angle between the outer and inner wings is too large, and the component of the aerodynamic force generated by the outer wing in the vertical direction decreases, so that the lift decreases. It can be seen from Figure 7b that the average thrust when the angle between outer and inner wings is negative is greater than that when the angle between outer and inner wings is positive. This is because when the angle between outer and inner wings is negative, the effective area of interaction with air in the upward process is larger, so that more thrust can be obtained. Through the curve, it is concluded that with the monotonic increase of the angle between the outer and inner wings, the average thrust also monotonically decreases. It can be seen from Figure 7c that the average pitch moment (Absolute value) when the angle between outer and inner wings is negative is greater than that when the angle between outer and inner wings is positive. Through the curve, it is concluded that with the monotonic increase of the angle between the outer and inner wings, the average pitch moment also monotonically decreases.

In summary, as the angle between the outer and inner wings increases, the lift initially rises but then starts to decrease. When the angle is near 15°, the maximum lift can be obtained. The thrust and pitch moment decreases with the increase of the angle between the outer and inner wings.

4. WIND TUNNEL EXPERIMENT

To ensure the correctness of the analysis conclusion, it is necessary to ensure the accuracy of the simulation. Therefore, wind tunnel experiments are used to verify the accuracy of the simulation. The devices placed into the wind tunnel for experiment includes: flapping-wing robot prototype, a six-component force sensor, and a fixed bracket. The model of the prototype chooses the angle between the outer and inner wings of 0° and 15° for comparison experiment. The parameters of the wind tunnel and the motion parameters of the prototype are the same as those of the simulation experiment. Figure 8 shows the motion of the prototypes in the wind tunnel.

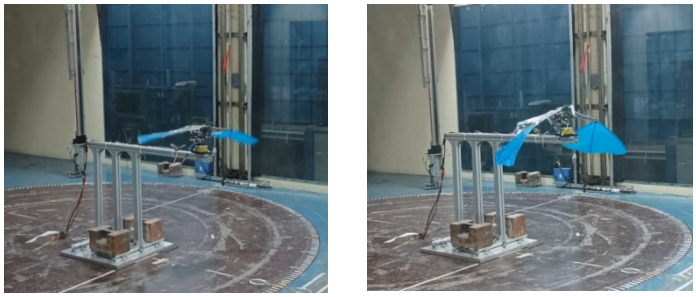

(a) The outer and inner wings of 0° (b) The outer and inner wings of 15°

Figure 8. The motion of the prototypes in the wind tunnel.

Figure 9 shows the aerodynamic data collected by the prototype with the angle of 0°. Among them, the blue curve is the original data, the red curve is the smooth curve after filtering, and the green curve is the average data after averaging the data. Similarly, the data with an angle of 15° between the outer and inner wings are processed the same.

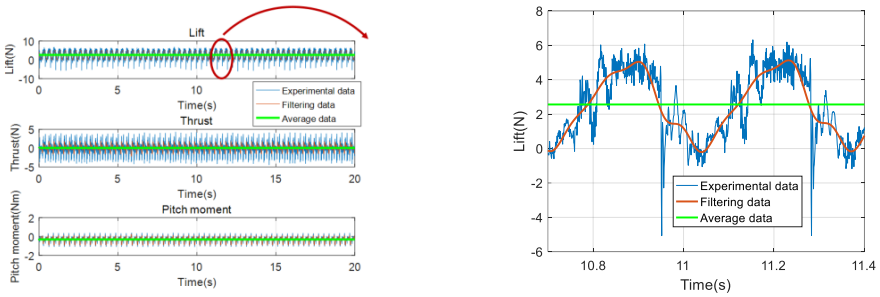

(a) Aerodynamic force curves before and after filtering (b) Local amplification curve of lift force

Figure 9. The aerodynamic data with the angle of 0° between the outer and inner wings in the wind tunnel.

Through the wind tunnel experiment, when the angle between the outer and inner wings is 0°, the average lift is 2.564 N, while the simulation result is 2.480 N, and the error between the two is 3.28 %; and when the angle between the outer and inner wings is 15°, the average lift is 2.829 N, while the simulation result is 2.732 N, and the error between the two is 3.55 %, the errors are within the acceptable range. In addition, the simulation data show that the lift of the wing with the outer and inner wings angle of 15° is 10.16% higher than that with the angle of 0°, when the wind tunnel experimental shows the improvement is 10.34%, and the lift improvement ratio is almost the same, which can prove the correctness of the simulation results.

5. CONCLUSION

The purpose of this paper is to explore the effect of the angle between the outer and inner wings of FAV on the aerodynamic characteristics of the wings. The structural analysis of the outer and inner wings is carried out, and a series of wing models with different angles between the outer and inner wings are established. The aerodynamic forces of the wings under different angles between the outer and inner wings are obtained by the co-simulation of XFlow-Abaqus and wind tunnel experiment. Through the analysis of the results, the following conclusions are summarized:

(1) The lift exhibits an initial increase followed by a decrease as the angle between the outer and inner wings is increased. When the angle is near 15°, the maximum lift can be obtained, and the lift is about 10% higher than that of with the angle of 0°. Therefore, when the lift of FAV is insufficient, the angle can be changed to 15° to meet the flight requirements.

(2) The thrust decreases with the increase of the angle between the outer and inner wings. So, when FAV needs to improve thrust, it can reduce the angle to improve thrust.

(3) The pitch moment decreases with the increase of the angle between the outer and inner wings. Therefore, when the FAV is unstable, the angle can be appropriately increased to reduce the pitch moment and improve the stability.

The research in this paper can provide theoretical guidance for the wing structure optimization of flapping wing robots, so as to achieve the optimal aerodynamic characteristics of wings with the same mass, the same movement law, the same structural parameters and the same wing area, and improve the flight performance of flapping wing robots.

ACKNOWLEDGEMENT

This work was supported by the National Natural Science Foundation of China (Grant No.52175521), National Key R&D Program of China (Grant No.2022YFB3403602), and the Fundamental Research Funds for the Central Universities.

REFERENCES

[1] Gerdes, J. W., Gupta, S. K. and Wilkerson, S. A., “A review of bird-inspired flapping wing miniature air vehicle designs,” Journal of Mechanisms and Robotics-Transactions of the ASME 4, 21003 (2012).

[2] Keennon, M., Klingebiel, K. and Won, H., "Development of the nano hummingbird: A tailless flapping wing micro air vehicle," 50th AIAA Aerospace Sciences Meeting including the New Horizons Forum and Aerospace Exposition, (2012).
[3] Han, J. K., Hui, Z., Tian, F. B., et al., "Review on bio-inspired flight systems and bionic aerodynamics," Chinese Journal of Aeronautics 34, 170-186 (2020).
[4] Huang, H., He, W., Wang, J. B., et al., "An all servo-driven bird-like flapping-wing aerial robot capable of autonomous flight," IEEE/ASME Transactions on Mechatronics 27(6), 5484-5494 (2022).
[5] Jafferis, N. T., Helbling, E. F., Karpelson, M. and Wood, R. J., "Untethered flight of an insect-sized flapping-wing microscale aerial vehicle," Nature 7762(570), 491-495 (2019).
[6] Karásek, M., Muijres, F. T., De Wagter, C., et al., "A tailless aerial robotic flapper reveals that flies use torque coupling in rapid banked turns," Science 6407(361), 1089-1094 (2018).
[7] Fei, F., Tu, Z., Yang, Y., et al., "Flappy hummingbird: an open-source dynamic simulation of flapping wing robots and animals," IEEE International Conference on Robotics and Automation (ICRA) 9223-9229 (2019).
[8] Ramezani, A., Chung, S. J. and Hutchinson, S., "A biomimetic robotic platform to study flight specializations of bats," Science Robotics 3(2), eaal2505 (2017).
[9] Chang, E, Matloff, L. Y., Stowers, A. K., et al., "Soft biohybrid morphing wings with feathers underactuated by wrist and finger motion," Science Robotics 5(38), eaay1246 (2020).
[10] Zufferey, R., Barbero, J. T., Garcia, M., et al., "Design of the high-payload flapping wing robot E-Flap," IEEE Robotics and Automation Letters, (2021).
[11] Ang, H. S., Xiao, T. H. and Duan, W. B., "Flight mechanism and design of biomimetic micro air vehicles," Science in China Series E 52(13), 3722-3728 (2009).
[12] Huang, M., "Optimization of flapping wing mechanism of bionic eagle," Proceedings of the Institution of Mechanical Engineers 233(9), 3260-3272 (2019).
[13] Mahardika, N., Viet, N. Q. and Park, H. C., "Effect of outer wing separation on lift and thrust generation in a flapping wing system," Bioinspiration & Biomimetics 6(3), 036006 (2011).
[14] Norberg, U. M. and Rayner, J. M. V., "Ecological morphology and flight in bats (Mammalia; Chiroptera): Wing adaptations, flight performance, foraging strategy and echolocation," Philosophical Transactions of the Royal Society B: Biological Sciences 316(1179), 335-427 (1987).